Published in final edited form as:
J Immunol. 2011 November 15; 187(10): 5419–5428. doi:10.4049/jimmunol.1101267.

IFNγ promotes muscle damage in the *mdx* mouse model of Duchenne muscular dystrophy by suppressing M2 macrophage activation and inhibiting muscle cell proliferation

S. Armando Villalta[*], **Bo Deng**[*], **Chiara Rinaldi**[†], **Michelle Wehling-Henricks**[†], and **James G. Tidball**[*,†,‡]

[*]Molecular, Cellular & Integrative Physiology Program, University of California, Los Angeles, CA

[†]Department of Integrative Biology and Physiology, University of California, Los Angeles, CA

[‡]Department of Pathology and Laboratory Medicine, David Geffen School of Medicine at UCLA, University of California, Los Angeles, CA

Abstract

Duchenne muscular dystrophy is a degenerative disorder that leads to death by the third decade of life. Previous investigations have shown that macrophages that invade dystrophic muscle are a heterogeneous population consisting of M1 and M2 macrophages that promote injury and repair, respectively. In the present investigation, we tested whether interferon-γ (IFNγ) worsens the severity of *mdx* dystrophy by activating macrophages to a cytolytic, M1 phenotype and by suppressing the activation of pro-regenerative macrophages to a M2 phenotype. IFNγ is a strong inducer of the M1 phenotype and is elevated in *mdx* dystrophy. Contrary to our expectations, null mutation of IFNγ caused no reduction of cytotoxicity of macrophages isolated from *mdx* muscle and did not reduce muscle fiber damage *in vivo* or improve gross motor function of *mdx* mice at the early, acute peak of pathology. In contrast, ablation of IFNγ reduced muscle damage *in vivo* during the regenerative stage of the disease and increased activation of the M2 phenotype and improved motor function of *mdx* mice at that later stage of the disease. IFNγ also inhibited muscle cell proliferation and differentiation *in vitro* and IFNγ mutation increased MyoD expression in *mdx* muscle *in vivo*, showing that IFNγ can have direct effects on muscle cells that could impair repair. Together, the findings show that suppression of IFNγ signaling in muscular dystrophy reduces muscle damage and improves motor performance by promoting the M2 macrophage phenotype and by direct actions on muscle cells.

INTRODUCTION

Inflammatory cells can play central roles in determining the course of muscle injury and regeneration (1). The complexity and importance of interactions between muscle and the immune system for regulating muscle pathology has become increasingly apparent as our understanding of the pathology of muscular dystrophy grows, particularly in Duchenne muscular dystrophy (DMD) and the *mdx* mouse model of DMD. Although DMD and *mdx* dystrophies are caused by null mutations in the dystrophin gene that encodes a membrane-associated structural protein (2) and the primary defect causing muscle pathology is a weakened cell membrane (3), inflammatory cells play major roles in promoting the pathology. For example, depletion of macrophages from *mdx* muscle prior to the early acute onset of muscle fiber necrosis that occurs between 3 and 4 weeks of age (Figure 1) causes a

Correspondence: James G. Tidball, Molecular, Cellular & Integrative Physiology Program, University of California, Los Angeles, CA 90095-1606, Phone: 310-206-3395, FAX: 310-825-8489, jtidball@physci.ucla.edu.

70 to 80% reduction in muscle fiber injury (4). Likewise, other perturbations that diminish the inflammatory response in dystrophic muscle yield quantitatively similar reductions in muscle fiber damage (5 – 9). Those findings show that much of the muscle damage in dystrophin-deficiency is caused by inflammatory cells rather than by direct mechanical damage. That information has potential, therapeutic importance because it indicates that regulation of the immune response to dystrophic muscle damage could provide a valuable mechanism for reducing the pathology of muscular dystrophy.

Macrophages that cause muscle fiber damage in *mdx* dystrophy are a proinflammatory phenotype that is designated M1 macrophages (10). M1 macrophages can be driven to a state of classical activation by proinflammatory, Th1 cytokines, especially interferon-γ (IFNγ) and several findings suggest that IFNγ activation of *mdx* muscle macrophages can worsen the pathology of muscular dystrophy. For example, IFNγ expression is elevated in *mdx* muscles during the stage of the disease when macrophage-mediated muscle damage is rampant and numbers of M1 macrophages are greatly elevated (10). In addition, IFNγ stimulation of macrophages isolated from *mdx* muscles produces tremendous increases in their cytotoxicity toward muscle cells in vitro. However, whether IFNγ actually contributes to the pathophysiology of muscular dystrophy *in vivo* remains unknown.

Although beneficial effects of macrophage-depletion on *mdx* muscle pathology show that macrophages are important agents in worsening *mdx* dystrophy at the acute onset of the disease, more recent studies have shown that macrophages can also play significant roles in promoting muscle repair that occurs during the regenerative stage of *mdx* pathology. Muscle fiber damage is greatly attenuated in *mdx* mice between the ages of 4 and 12-weeks (4, 11), while myogenic cells respond to the acute onset of injury by entering the proliferative stage of development to expand their numbers, and then transitioning through early differentiation and terminal differentiation to generate new muscle fibers (12 – 14). In concert with the decline of damage and acceleration of regeneration, macrophage populations in *mdx* muscle transition from the proinflammatory, M1 phenotype to an anti-inflammatory M2 phenotype (10, 15) (Figure 1). Macrophages can be activated to an M2 phenotype by interleukin-4 (IL-4) and IL-13, which produce a state of alternative activation that is characterized by the production of anti-inflammatory cytokines (16, 17). Those anti-inflammatory cytokines include IL-10 that can deactivate M1 macrophages and further drive alternative activation. IL-10 plays a particularly important role in mediating this switch of macrophage phenotype in *mdx* muscle *in vivo* and reducing muscle damage caused by M1 macrophages (15). Ablation of IL-10 expression in *mdx* mice caused an increase in muscle damage in 12-week-old *mdx* mice and produced reductions in running endurance of *mdx* mice that coincided with the increases in muscle damage (15). Furthermore, macrophages that were stimulated with IL-10 increased proliferation of muscle cells in co-culture, showing that IL-10 can also increase muscle growth as well as reduce muscle damage through IL-10 mediated mechanisms (15).

Collectively, these studies show that modulating the relative activities or proportion of M1 and M2 macrophages in dystrophic muscle can influence the course and severity of the disease. Because of the important role of IFNγ in driving activation of monocytes and macrophages to the cytolytic, M1 phenotype, we anticipated that ablation of IFNγ could significantly reduce muscle damage in *mdx* dystrophy and provide a potential avenue for therapeutic interventions. We test that hypothesis in the present investigation by generating IFNγ null mutant *mdx* mice and assessing whether IFNγ promotes muscle fiber injury by activating M1 macrophages in *mdx* muscle. We measure the extent of muscle fiber injury during the acute and regenerative stages of dystrophinopathy in *mdx* and IFNγ-deficient mdx mice (IFNγ$^{-/-}$/*mdx*). In addition, we assay for changes in the cytotoxic potential of muscle macrophages isolated from *mdx* and IFNγ$^{-/-}$/*mdx* mice. We further test whether IFNγ

mediates a phenotypic shift toward an M1 phenotype by inducing M1 macrophages and suppressing the activation of M2 macrophages. We also evaluate if null mutation of IFNγ in *mdx* mice modulates muscle regeneration and investigate the effect of IFNγ on muscle cell proliferation and differentiation. Last, we assess whether perturbations in IFNγ expression in *mdx* muscle affect muscle function. Collectively, our findings provide novel information concerning the signals that drive the activation of macrophages in dystrophic muscle *in vivo* and provide insights into the effects of blocking IFNγ expression during muscular dystrophy. The results of this investigation suggest that disruptions of IFNγ signaling in muscles of DMD patients may reduce pathology by promoting the activation of anti-inflammatory, M2 macrophages. Furthermore, IFNγ blockade may enhance muscle regeneration during DMD and lead to preserved muscle function.

MATERIAL AND METHODS

Animals

C57BL/10ScSn-Dmd^{mdx}/J and B6.129S7-*Ifng*^{tm1Ts}/J mice were purchased from The Jackson Laboratory (Bar Harbor, ME) and bred in pathogen-free vivaria at the University of California, Los Angeles. B6.129S7-*Ifng*^{tm1Ts}/J mice were crossed onto the C57BL/6 background for at least 8 generations by the vendor. Mice carrying null mutation for IFNγ (B6.129S7-*Ifng*^{tm1Ts}/J mice) were crossed with *mdx* mice using the breeding strategy shown in Figure 2, to generate *mdx* mice that were null mutants for IFNγ (IFNγ$^{-/-}$/*mdx* mice) or background control *mdx* mice that expressed IFNγ. Null mutation of IFNγ was confirmed by PCR using primer sets specific for the wild-type allele (forward primer: 5′-AGA AGT AAG TGG AAG GGC CCA GAA G-3″; reverse primer: 5′-AGG GAA ACT GGG AGA GGA GAA ATA T-3′) and the neo cassette present in the mutant allele (forward primer: 5′-TCA GCG CAG GGG CGC CCG GTT CTT T-3′; reverse primer: 5′-ATC GAC AAG ACC GGC TTC CAT CCG-3′). Null mutation of the dystrophin gene was confirmed using *mdx*-amplification-resistant mutation system PCR (19). All animals were handled according to guidelines approved by the Chancellor's Animal Research committee at the University of California, Los Angeles.

Assay for muscle membrane lesions in vivo

Muscle membrane lesions were assessed by assaying for the presence of the extracellular matrix marker dye, procion orange, within muscle fibers (20). Procion orange was selected as a marker of membrane lesions because it is a vital dye that is not actively transported across cell membranes, instead entering through membrane lesions. After euthanasia, the solei of 4- and 12-week-old mice were dissected and incubated in 0.5% procion orange dye (Sigma) in Kreb's Ringer solution for 1 hour, followed by three, 5-minute rinses in Krebs' Ringer. The muscles were then rapidly frozen in liquid nitrogen-cooled isopentane. Cross-sections 10-μm thick were taken from the mid-belly of each soleus and viewed by fluorescence microscopy. Intracellular fluorescence intensity caused by dye influx was assayed within an 8-μm diameter, optical sampling circle by flourimetry using a microscope equipped with a digital imaging system (Bioquant, Nashville, TN). Fluorescence intensity was measured for every fiber present in complete cross-sections of entire mid-belly cross-sections of each soleus muscle. Measurements were corrected for background fluorescence measured at a site on the section that contained no tissue. Approximately 760 fibers were assayed in each muscle. Data were expressed as fluorescence intensity in arbitrary units and displayed graphically as the distribution frequency of fiber fluorescence in *mdx* mice or IFNγ$^{-/-}$/*mdx* mice.

Immunohistochemistry

Frozen, serial sections of 4- and 12-week-old mouse quadriceps were air-dried for 30 minutes and fixed in ice-cold acetone for 10 minutes. Sections were blocked for 1 hour with 3% bovine serum albumin (BSA) and 0.05 % Tween-20 diluted in 50 mM Tris-HCl pH 7.6 containing 150 mM NaCl. Sections were then probed with anti-IFNγ receptor-1 (IFNγR1; BD Bioscience, 1:20), anti-F4/80 (obtained by ammonium sulfate precipitation from HB-198 hybridoma cultures, ATCC) or anti-CD206 (Serotec) for 3 hours at room temperature. Sections were washed with PBS and then probed with biotin-conjugated secondary antibodies (Vector Laboratories, 1:200) for 1 hour at room temperature. Sections were subsequently washed with 50 mM sodium phosphate buffer pH 7.4 containing 200 mM sodium chloride (phosphate-buffered saline; PBS) and then incubated for 30 minutes with Avidin D-conjugated horseradish peroxidase (Vector Laboratories, 1:1000). Staining was visualized with the peroxidase substrate, 3-amino-9-ethylcarbazole (Vector Laboratories), yielding a red reaction product.

The numbers of immunolabeled inflammatory cells per unit volume of muscle were measured in muscle cross-sections using previously described morphometric techniques (4). The total number of either F4/80+ macrophages or CD206+ macrophages in each section was counted microscopically. The total volume of each section was determined by measuring the area of each section using a stereological, point-counting technique (4) and then multiplying that value by the section thickness (10 μm).

Muscle macrophage isolation

Muscle macrophages were isolated using a previously-described procedure (10). Hindlimb muscles of 4–6 mice were dissected and pooled in a 10 cm plate containing cold PBS. Muscles were cleared of discernible fat, rinsed with fresh PBS, and weighed. Dissected muscles were then minced to a fine pulp with surgical scissors and placed into 50 ml conical tubes, which received 10 ml per gram muscle mass of collagenase Type IV (1.0 mg/ml) in Dulbecco's modified Eagle's medium (DMEM). Tubes were incubated in a rotary incubator at 37°C for two 45-minute periods. After the initial 45 minutes of collagenase treatment, undigested muscle was allowed to settle for 2 minutes. The resulting cell suspension was aspirated, centrifuged in 50 ml conical tubes at 850 g, and resuspended with PBS. The remaining undigested muscle was further digested in fresh collagenase buffer for a second 45-minute period, after which the cell suspensions were centrifuged, resuspended, and pooled with cells from the first 45-minute digestion. Pooled single-cell suspensions were then filtered through a 70-μm cell strainer and subsequently centrifuged at 850 g for 5 minutes. Filtered, single-cell suspensions were then applied to 15 ml of Histopaque 1077 and centrifuged at 1000 g for 30 minutes. Cells were collected from the Histopaque and DMEM interface, washed with complete DMEM, and counted. Approximately 80% of the cells collected from the interface were F4/80 positive.

Macrophage-mediated cytotoxicity assay

Macrophage-mediated cytotoxicity was assessed with a previously reported assay (4, 10). 96-well plates were seeded with 15,000 C_2C_{12} cells per well in complete medium (DME; Dulbecco's minimal essential medium containing 10% fetal bovine serum, and 1% penicillin and streptomycin) and allowed to reach confluency before overnight serum starvation to trigger fusion. Following serum starvation, cells were returned to complete medium to differentiate for 3 days. Prior to co-culturing with muscle macrophages, myotubes were incubated with 0.4% ^{51}Cr in HBSS assay buffer (Hank's buffer saline solution containing 0.25 % FBS and 400 μM L-arginine) for 2 hours. Muscle macrophages isolated from *mdx* and IFNγ$^{-/-}$/*mdx* mice were cocultured with ^{51}Cr-treated myotubes at concentrations of 5×10^5, 6×10^5 or 7×10^5 macrophages/well in 150 μl of HBSS assay buffer, using 96-well

plates. Following 24 hours of co-culturing, 75 μl of media were collected from each well and ^{51}Cr release was measured using a Beckman Gamma 5500 liquid scintillation counter. Cytotoxicity was expressed as a percentage of total lysis by setting 0% as ^{51}Cr released spontaneously by myotubes cultured without macrophages. 100% cytotoxicity was set as the ^{51}Cr released into the media by myotubes incubated with 0.1% Triton X-100 in HBSS assay buffer.

Western blot analysis

The expression levels of iNOS, MyoD and myogenin were assayed by western blot analysis. Equal loading of samples was determined by staining nitrocellulose blots with 0.1% Ponceau S solution (Sigma-Aldrich). Nitrocellulose membranes blocked with 3% milk were probed with rabbit antibodies against mouse iNOS (Upstate Biotechnology, 1:300) for 3 hours at room temperature. Membranes were then washed with PBS containing 0.05% Tween-20 and probed with horseradish peroxidase (HRP) conjugated-donkey anti-rabbit IgG (Amersham, 1:10,000) for one hour at room temperature. Membranes were washed and the expression levels of iNOS were visualized with chemiluminescent substrate and a fluorochem imaging system (Alpha Innotech). The imaging system was also used to assess relative expression levels of iNOS according to relative fluorescent signal intensities for iNOS bands in the membranes. Blots were similarly probed for relative quantities of MyoD or myogenin using mouse anti-MyoD (BD Bioscience, 1:150) or mouse anti-myogenin (BD Bioscience, 1:150) and HRP-conjugated anti-mouse IgG secondary antibody.

RNA isolation and quantitative PCR

Frozen muscles were homogenized with a mortar and pestle while partially submerged in liquid nitrogen. One milliliter of Trizol (Invitrogen) per 50 mg of tissue was pipetted directly into the mortar and pestle and further homogenized while in liquid nitrogen. The resulting homogenized powder was thawed and transferred to 2 ml centrifuge tubes and RNA extracted according the manufacturer's protocol (Invitrogen). RNA from freshly-isolated muscle macrophages was isolated with RNeasy spin columns (Qiagen). Muscle and macrophage RNA samples were further cleaned and DNase-treated using RNeasy spin columns according the manufacturer's protocol. Five hundred nanograms of total RNA were reverse transcribed with Super Script Reverse Transcripase II using oligo dTs to prime extension (Invitrogen). The resulting cDNA was used to measure quantitatively the expression of genes involved in classical and alternative activation using SYBR green qPCR master mix according the manufacturer's protocol (BioRad).

Real-time measurements of gene expression were performed with an iCycler thermocycler system and iQ5 optical system software (BioRad). cDNA resulting from reverse transcription PCR was used to measure the expression of genes associated with M1 and M2 macrophages using SYBR green qPCR master mix according to the manufacturer's protocol (BioRad). Primers used for PCR to assay relative levels of expression of muscle-specific and immune-cell specific genes are shown in Table 1. We determined empirically reference genes that did not vary between the experimental groups in our investigation by assaying nine reference genes in murine skeletal muscle using geometric averaging (geNorm Visual Basic version 3.5; reference 21). Primers used for PCR to assay expression levels of reference genes are shown in Table 2. After identifying the most stable genes between the groups analyzed, we assayed the ideal number of reference genes for normalization and determined that 2 genes were sufficient for reliable normalization. Based on this assessment, TPT1 and RPL13A were selected as reference genes for data normalization.

Assessment of muscle fiber regeneration

Muscle fibers that have experienced injury and repair contain centrally-located nuclei, which provide a morphological indicator of fibers that are undergoing regeneration (41). The percentage of total muscle fibers containing central nuclei that were present in complete cross-sections of entire soleus muscles stained with hematoxylin was determined by light microscopy.

Muscle cell proliferation assay

A previously reported flow cytometry-based assay was used to study the effect of IFNγ on muscle cell proliferation (23, 24). GFP-expressing C_2C_{12} cells were labeled with the membrane-intercalating dye, CellVue Claret, according the manufacturer's instructions. After labeling, 200,000 cells were plated in tissue culture plates (BD Bioscience) with complete media and cultured at 37°C and 5% CO_2. After 72 hours of culturing in the presence or absence of IFNγ (10 ng/ml), cells were detached with a 0.05% solution of trypsin-EDTA and fluorescence intensity analyzed with a Becton-Dickson FACSCalibur flow cytometry. C_2C_{12} cells grown in serum free conditions served as a nonproliferative population, which retained high fluorescence intensity of CellVue Claret labeling. Increases in muscle cell proliferation were reflected by an increase in the proportion of cells with low fluorescence intensity (CellVue Claret^{low} cells).

Assessment of muscle function

i. Running protocol—Mice ran on an Exer 3/6 treadmill (Columbus Instruments) containing a shock grid that stimulated mice to run at a speed of 8 m/min with a 5° incline. The shock stimulus was provided at an intensity of 3.4 milliamperes for 200 milliseconds at 3 Hz. The end run-time was recorded when a mouse stopped to rest for a period of 10 continuous seconds on the shock grid. Mice were run for a maximum of 60 minutes. Data are expressed as the mean maximum running time of 20 mice per group.

ii. Wire hang test—We used a variation of a wire-hang test to assess the effect of IFNγ null mutation on muscle function and strength (15, 25). Three trials for each mouse were performed and data were expressed as the mean hang-time of the averaged trial times of 15–20 mice tested. In order to allow mice to recover and minimize fatigue and distress, mice were allowed to rest for one minute between trials.

Statistics

Statistical analysis was performed in InStat version 2.03 (GraphPad Software). For multi-factorial comparisons, we performed a Kruskal-Wallis test to determine statistical significance, followed by a post-hoc student *t*-test to determine significance of differences between two groups. Significance was accepted at $p < 0.05$.

RESULTS

IFNγ promotes muscle fiber damage during the regenerative stage of mdx dystrophy

Assays of muscle membrane lysis in 4- and 12-week-old *mdx* soleus muscles show that IFNγ increases muscle membrane damage during the regenerative stage of dystrophinopathy. Fluorescence intensity of the cytosol of muscle fibers in soleus muscles incubated with procion orange did not differ between 4-week-old *mdx* and IFNγ$^{-/-}$/*mdx* mice, indicating that IFNγ–mediated processes do not contribute to muscle fiber injury during the acute, degenerative stage of dystrophinopathy (Figure 3A). However, ablation of the IFNγ gene in 12-week-old *mdx* mice reduced cytosolic fluorescence, suggesting that IFNγ either promotes chronic muscle fiber injury or prevents repair (Figures 3B–H). We

then tested whether the reduction of fiber damage in 12-week-old, IFNγ$^{-/-}$/*mdx* mice reflected lower concentrations of macrophages in muscles and found that macrophage numbers in *mdx* muscle declined between 4 and 12 weeks of age, but macrophage numbers did not differ between *mdx* and IFNγ$^{-/-}$/*mdx* mice at either 4 or 12 weeks of age (Figure 3I). We then assayed whether the macrophages isolated from 12-week-old, IFNγ$^{-/-}$/*mdx* mice were less cytotoxic than macrophages in *mdx* muscles from mice that expressed IFNγ but found that macrophages from 12-week-old *mdx* and IFNγ$^{-/-}$/*mdx* mice did not differ in their lysis of myotubes when tested in cytotoxicity assays performed *in vitro* (Figure 3J). Collectively, these data show that IFNγ-mediated events contribute to *mdx* muscle damage between 4 and 12-weeks of age, but that the IFNγ-driven damage is not attributable to increases in the numbers or cytotoxicity of muscle macrophages.

Null mutation of IFNγ in mdx mice increases macrophage activation to the M2 phenotype during the regenerative stage of mdx dystrophy

Expression levels of mRNA and proteins associated with M1 macrophage activation were assayed to determine whether IFNγ deficiency in *mdx* mice affected macrophage phenotype in dystrophic muscle. Expression of iNOS by macrophages is the quintessential marker of M1 activation, but quantitative, real-time PCR (qPCR) showed no significant difference in iNOS mRNA levels in muscles of 4-week-old or 12-week-old *mdx* and IFNγ$^{-/-}$/*mdx* mice (Figure 4A). However, ablation of IFNγ in *mdx* mice at either age caused significant reductions in macrophage iNOS at the protein level, supporting a role for IFNγ in promoting M1 activation in muscle macrophages at the post-translational level (Figure 4B, C). Despite the finding that IFNγ ablation reduced iNOS in *mdx* muscle, IFNγ ablation did not affect the expression of other markers that reflect M1 macrophage activation, including IL-6, IP-10 and MCP-1. Furthermore, IFNγ$^{-/-}$/*mdx* mice showed higher levels of expression of TNFα relative to expression in *mdx* muscles (Figure 4D).

Changes in expression levels for transcripts that are associated with M2 macrophage activation were also assessed by qPCR. Mutation of IFNγ in *mdx* mice caused a significant increase in expression of all genes associated with M2 macrophages that were assayed, including arginase-1, arginase-2, FIZZ-1, Mgl-2, CD206 and IL-4 (Figure 5A). The elevations of arginase expression, which increased 3- to 4-fold in 12-week-old IFNγ$^{-/-}$/*mdx* muscles, may be of particular functional importance because arginase activity promotes wound healing following tissue damage (26 – 28). Perhaps most significantly, the expression of CD206, the most widely-accepted and specific marker of alternative activation of M2 macrophages (17, 29), more than doubled in 12-week-old IFNγ$^{-/-}$/*mdx* muscles compared to age-matched mdx muscles. Quantitative immunohistochemical data also showed that ablation of IFNγ expression in *mdx* mice caused a significant increase in the number of CD206+ cells in 12-week-old *mdx* muscle (Figure 5B). Notably, the magnitude of the increase in CD206 expression in 12-week-old IFNγ$^{-/-}$/*mdx* muscles compared to 12-week-old *mdx* muscles (Figure 5A) was greater than the magnitude of the increase in the numbers of CD206+ macrophages in 12-week-old IFNγ$^{-/-}$/*mdx* muscles (Figure 5B). This may be attributable to the increase in the level of expression of CD206 per M2 macrophage, which was evident in immunohistochemical assays (Figure 6). Collectively, these findings indicate that IFNγ is a strong negative regulator of macrophage activation to the M2 phenotype and may potentially slow muscle repair during the regenerative stage of *mdx* dystrophy.

IFNγ inhibits muscle cell proliferation and differentiation in vitro

Because our immunohistochemical observations showed that the expression of the IFNγ receptor at the surface of muscle cells is greater in 4- and 12-week-old *mdx* mice compared to C57 control mice (Figure 7A–D), we tested whether IFNγ influenced muscle proliferation

or differentiation or affected the regeneration of *mdx* muscle. We used a flow cytometry-based assay to measure proliferation of green fluorescent protein-(GFP)-expressing C_2C_{12} cells in the presence or absence of IFNγ. In this technique, fluorescent membrane-intercalating dyes in cells undergoing division are partitioned between newly-generated daughter cells. As a result, the fluorescence intensity of daughter cells is reduced compared to the initially-stained parent cells (23). C_2C_{12} myoblasts expressing GFP that were grown in serum-free conditions that attenuated cell proliferation showed high fluorescence intensity with the fluorescent membrane-intercalating dye (CellVue Claret; reference 23). Lower fluorescence intensity was observed when the cells were grown in growth media, which promotes muscle cell proliferation (Figure 7E). However, IFNγ treatment of muscle cells for 72 hours showed higher fluorescence intensity of muscle cells grown in growth media, indicating an inhibition in muscle cell proliferation (Figure 7E). Unexpectedly, we also found that IFNγ treatment of muscle cells *in vitro* reduced the expression of myogenin, but not MyoD (Figure 7F). Because myogenin expression is elevated during transition of muscle cells from the proliferative stage to the early differentiation stage of development, these findings suggest IFNγ can inhibit muscle differentiation. Morphological observations also supported a role for IFNγ in inhibiting muscle differentiation and growth. Addition of IFNγ to C_2C_{12} cultures after their transfer from complete media to media containing 2% normal horse serum only showed that the myotubes that differentiated in the presence of IFNγ were substantially smaller than those that differentiated in the absence of IFNγ (Figure 7G).

IFNγ deficiency in mdx mice increases MyoD expression during regeneration

Assays of MyoD expression in muscles of *mdx* and IFNγ$^{-/-}$/*mdx* mice also indicate a role for IFNγ in influencing muscle cell proliferation or differentiation *in vivo*. The qPCR data show that MyoD levels are significantly higher in IFNγ$^{-/-}$/*mdx* muscle than in *mdx* muscle at 12 weeks (Figure 7H), which may reflect larger numbers of activated satellite cells in the muscle. Expression levels of myogenin also tended to be higher in IFNγ$^{-/-}$/*mdx* muscle than in *mdx* muscle at 12 weeks (Figure 7I), although the difference did not reach statistical significance. However, this perturbation of the normal proliferation or differentiation of *mdx* muscle that was caused by IFNγ mutation did not have an apparent effect on regeneration at 12-weeks; the increase in muscle fiber central-nucleation that occurred between 4 and 12-weeks did not differ between *mdx* and IFNγ$^{-/-}$/*mdx* muscles (Figure 7J).

IFNγ contributes to muscle dysfunction in mdx dystrophy

Running time until fatigue was measured for *mdx* and IFNγ$^{-/-}$/*mdx* to test whether the decrease in muscle fiber damage that occurred in IFNγ$^{-/-}$/*mdx* mice was reflected in improved running performance. Running time did not differ between *mdx* and IFNγ$^{-/-}$/*mdx* mice at 4-weeks of age (Figure 8A), which corresponded to lack of difference in muscle fiber injury that was observed at that age (Figure 3A). However, the running time for 12-week-old IFNγ$^{-/-}$/*mdx* mice was 230% greater than the time for age-matched, *mdx* mice (Figure 8A), which was consistent with the decreased muscle fiber injury in IFNγ$^{-/-}$/*mdx* mice at this age (Figure 3B). No difference in hang time was observed at either 4 or 12 weeks of age between *mdx* and IFNγ$^{-/-}$/*mdx* mice (Figure 8B).

DISCUSSION

The findings in the present investigation generally support our hypothesis that disruption of IFNγ-mediated signaling in dystrophic muscle would decrease the pathophysiology of muscular dystrophy. The reductions in pathology were evident at the gross level, where ablation of IFNγ in *mdx* mice caused more than a doubling of treadmill running time, and also at the histological level, where deletion of IFNγ caused significant reductions in muscle fiber injury. Our data also show that the beneficial effects of IFNγ mutation could be

mediated through more than one pathway. IFNγ mutation affected the balance in M1 and M2 macrophage populations in *mdx* muscle, causing a shift to the M2 phenotype that can promote muscle growth and repair following injury. However, our findings show that the beneficial effects of IFNγ deletion may also reflect a loss of direct effects on muscle cells, through which IFNγ can inhibit proliferation of myogenic cells and delay their differentiation. Each of these beneficial effects of IFNγ mutation on the pathology of *mdx* dystrophy were apparent at 12-weeks of age, when levels of *mdx* fiber damage are relatively low and muscle regeneration is a prominent component of the pathology.

Although our findings show clear, beneficial effects of ablating IFNγ in 12-week-old *mdx* mice, we were surprised to learn that blocking IFNγ signaling does not affect muscle fiber injury during the acute, degenerative stage at 4-weeks of age or influence gross motor function in 4-week-old *mdx* mice. We anticipated a positive treatment effect in 4-week-old mice because previous studies showed that muscle macrophages isolated from 4-week-old *mdx* mice are predominantly M1-activated and they are more cytotoxic than macrophages isolated from 12-week-old *mdx* muscles (10). Furthermore, IFNγ stimulation of muscle macrophages that were isolated from 4-week-old *mdx* mice increased their cytotoxicity and IFNγ expression in 4-week-old *mdx* muscles is higher than in wild-type controls (10). Nevertheless, IFNγ deletion did not affect the cytotoxicity of macrophages that were isolated from *mdx* muscles and did not reduce *mdx* muscle fiber damage at 4-weeks of age and produced only small reductions in iNOS expression by muscle macrophages isolated from 4-week-old *mdx* mice. Together, the findings show that M1 macrophage cytotoxicity at the early, acute stage of *mdx* pathology is primarily driven by factors other than IFNγ. Although TNFα would have been a candidate cytokine for promoting M1 activation in *mdx* muscle because it has the capacity to promote M1 activation and cytotoxicity (29) and its expression is elevated in *mdx* muscle (30), our current findings do not support that role for TNFα in *mdx* dystrophy. On the contrary, ablation of IFNγ caused significant increases in TNFα expression in 12-week-old muscle, while muscle fiber damage declined. Furthermore, and perhaps of broader significance, our finding that muscle macrophages from 4-week-old IFNγ$^{-/-}$/*mdx* mice exhibited the M1 phenotypic characteristic of elevated iNOS expression shows that IFNγ is not required for classical activation of macrophages, at least in muscular dystrophy. This observation is contrary to the canon that IFNγ is required to condition macrophages for classical activation (29).

Although previous investigations have shown that IFNγ is a strong inducer of the M1 macrophage phenotype, its role in promoting *mdx* pathology appears to be more directly attributable to its suppression of the M2 phenotype. In addition to the ineffectiveness of IFNγ ablation for reducing muscle damage caused by M1 macrophages, IFNγ mutation did not have a uniform effect on suppressing markers of M1 activation *in vivo*. On the contrary, loss of IFNγ nearly doubled the expression of TNFα, which typically reflects Th1 inflammatory responses that include elevated numbers of M1 macrophages, while having no effect on the expression levels of other genes associated with the M1 phenotype. In contrast, IFNγ mutation in 12-week-old *mdx* mice produced either significant elevations of all transcripts associated with M2 activation, suggesting that IFNγ expression in 12-week-*mdx* muscle is a strong suppressor of the M2 phenotype, but insufficient for classical activation of the M1 phenotype. As shown in previous work, that suppression of the M2 phenotype would increase muscle damage by diminishing M2 macrophage inhibition of M1 macrophage cytotoxicity. In particular, M2 macrophages in *mdx* muscles express arginase that hydrolyses arginine (10, 31), thereby depleting arginine availability for iNOS. This substrate competition leads to a reduction in NO production by M1 macrophages and a suppression of M1 macrophage cytotoxicity (10). Thus, IFNγ suppression of the M2 phenotype reduces substrate competition for arginine by arginase, increasing arginine

availability for iNOS in M1 macrophages and thereby increasing iNOS-mediated pathology without induction of the M1 phenotype or promoting iNOS expression.

Some of the beneficial effects of IFNγ on *mdx* pathology at 12-weeks of age may also reflect the removal of negative influences that IFNγ exerts on the regenerative process through both direct and indirect actions on muscle. We found that IFNγ acts directly on muscle cells *in vitro* and inhibits the proliferation of C_2C_{12} myoblasts, which is consistent with previous reports that IFNγ also inhibits the proliferation of human myoblasts (32). However, other investigators showed previously that treating myoblasts *in vitro* with neutralizing antibodies to the IFNγ receptor reduced C_2C_{12} proliferation (33), suggesting that IFNγ promotes rather than inhibits proliferation. However, these results are not necessarily in conflict. Levels of endogenous IFNγ production by muscle are much lower than levels that occur in inflamed muscle and previous investigators have shown a dose-dependency on the effects of IFNγ on muscle proliferation. Low concentrations of IFNγ (1–100 U/ml) increase muscle cell proliferation (34), whereas stimulation of myoblasts with high doses of IFNγ (>1000 U/ml) inhibits proliferation (35). We also observed that IFNγ treatment of muscle cells *in vitro* reduced the concentration of myogenin and decreased cell fusion, without affecting levels of MyoD expression, indicating that inhibition of differentiation is a direct effect on muscle cells. However, IFNγ deficiency in *mdx* mice caused an increase in MyoD expression at 12 weeks. This finding of an IFNγ-mediated effect on MyoD expression *in vivo* in the absence of an effect *in vitro* may reflect an indirect influence, possibly through IFNγ induction of a suppressor of MyoD expression by a non-muscle cell type.

The complex picture that is emerging from studies of the interactions between inflammatory cells and muscle in muscular dystrophy shows that broad approaches to attenuating the inflammatory response are likely to have negative effects in addition to the desired and expected positive effects on the pathophysiology. As emphasized by the present study and other investigations (36 – 40), use of non-specific anti-inflammatory drugs or other immunosuppressants could reduce inflammatory cell-mediated damage, but could also suppress pro-regenerative effects of immune cells. Furthermore, interventions that are intended to reduce inflammatory cell involvement in muscular dystrophy can also have direct deleterious effects on muscle cells. For example, cyclosporine A has been used for the treatment of DMD in which it was intended to suppress immune cell involvement in the disease (41). However, cyclosporine A is not an anti-inflammatory, *per se*. Cyclosporin A is an inhibitor of calcineurin that mediates many signaling pathways in multiple cell types, including muscle cells. For example, calcineurin activation is essential for normal patterns of gene expression during muscle adaptation (42) and blocking calcineurin signaling with cyclosporine A prevents muscle growth in response to increased muscle loading (43, 44). Thus, its application to DMD patients could impair the regenerative capacity of the muscle, even while reducing inflammation, to yield a net increase in muscle pathology. Finally, as illustrated by the current findings, the efficacy and mechanism of action of immune-based interventions can change with the stage of the disease at which the treatments are applied. Because the composition of the immune cell infiltrate in dystrophic muscle varies during the course of the disease and the effector molecules such as cytokines that are produced by inflammatory cells are pleiotropic proteins, the efficacy of immune-based interventions in DMD will likely be specific to the stage of the pathology. Thus, future immune-based strategies for treating muscular dystrophy can be improved by targeting specific immune cell populations and by applying the interventions at carefully selected stages of the disease.

Acknowledgments

This work was supported by grants from Muscular Dystrophy Association, USA (#157881 and #4031) and the National Institutes of Health (R01 AR47721, RO1 AR47855, R01 AR/AG054451) to J.G.T. and F31 AR054724to S.A.V.

We thank Erin Tricker for generating the GFP-expressing C_2C_{12} cell line. The authors also thank Miguel Angel Gutierrez for technical assistance.

References

1. Tidball JG, Villalta SA. Interactions between muscle and the immune system regulate muscle growth and regeneration. Amer J Physiol. 2010; 298:R1173–1187.
2. Hoffman EP, Brown RH Jr, Kunkel LM. Dystrophin: the protein product of the Duchenne muscular dystrophy locus. Cell. 1987; 51:919–928. [PubMed: 3319190]
3. Petrof BJ, Shrager JB, Stedman HH, Kelly AM, Sweeney HL. Dystrophin protects the sarcolemma from stresses developed during muscle contraction. Proc Natl Acad Sci U S A. 1993; 90:3710–3714. [PubMed: 8475120]
4. Wehling M, Spencer MJ, Tidball JG. A nitric oxide synthase transgene ameliorates muscular dystrophy in *mdx* mice. J Cell Biol. 2001; 155:123–131. [PubMed: 11581289]
5. Wehling-Henricks M, Lee JJ, Tidball JG. Prednisolone decreases cellular adhesion molecules required for inflammatory cell infiltration in dystrophin-deficient skeletal muscle. Neuromuscul Disord. 2004; 14:483–490. [PubMed: 15336689]
6. Acharyya S, Villalta SA, Bakkar N, Bupha-Intr T, Janssen PM, Carathers M, Li ZW, Beg AA, Ghosh S, Sahenk Z, Weinstein M, Gardner KL, Rafael-Fortney JA, Karin M, Tidball JG, Baldwin AS, Guttridge DC. Interplay of IKK/NF-kappaB signaling in macrophages and myofibers promotes muscle degeneration in Duchenne muscular dystrophy. J Clin Invest. 2007; 117:889–901. [PubMed: 17380205]
7. Whitehead NP, Pham C, Gervasio OL, Allen DG. N-Acetylcysteine ameliorates skeletal muscle pathophysiology in *mdx* mice. J Physiol. 2008; 586:2003–2014. [PubMed: 18258657]
8. Li H, Mittal A, Makonchuk DY, Bhatnagar S, Kumar A. Matrix metalloproteinase-9 inhibition ameliorates pathogenesis and improves skeletal muscle regeneration in muscular dystrophy. Hum Mol Genet. 2009; 18:2584–2598. [PubMed: 19401296]
9. Kumar A, Bhatnagar S, Kumar A. Matrix metalloproteinase inhibitor batimastat alleviates pathology and improves skeletal muscle function in dystrophin-deficient *mdx* mice. Am J Pathol. 2010; 177:248–260. [PubMed: 20472898]
10. Villalta SA, Nguyen HX, Deng B, Gotoh T, Tidball JG. Shifts in macrophage phenotypes and macrophage competition for arginine metabolism affect the severity of muscle pathology in muscular dystrophy. Hum Mol Genet. 2009; 18:482–496. [PubMed: 18996917]
11. Cullen MJ, Jaros E. Ultrastructure of the skeletal muscle in the X chromosome-linked dystrophic (*mdx*) mouse. Comparison with Duchenne muscular dystrophy. Acta Neuropathol. 1988; 77:69–81. [PubMed: 3239377]
12. Jin Y, Murakami N, Saito Y, Goto Y, Koishi K, Nonaka I. Expression of MyoD and myogenin in dystrophic mice, *mdx* and *dy*, during regeneration. Acta Neuropath. 2000; 99:619–627. [PubMed: 10867795]
13. Sabourin LA, Rudnicki MA. The molecular regulation of myogenesis. Clinical Genet. 2000; 57:16–25. [PubMed: 10733231]
14. Lluís F, Perdiguero E, Nebreda AR, Munoz-Canovez P. Regulation of skeletal muscle gene expression by p38 MAP kinases. Trends Cell Biol. 2006; 16:36–44. [PubMed: 16325404]
15. Villalta SA, Rinaldi C, Deng B, Liu G, Fedor B, Tidball JG. Interleukin-10 reduces the pathology of *mdx* muscular dystrophy by deactivating M1 macrophages and modulating macrophage phenotype. Hum Mol Genet. 2011; 20:790–805. [PubMed: 21118895]
16. Mantovani A, Sica A, Sozzani S, Allavena P, Vecchi A, Locati M. The chemokine system in diverse forms of macrophage activation and polarization. Trends Immunol. 2004; 25:677–686. [PubMed: 15530839]

17. Gordon S. Alternative activation of macrophages. Nature Rev. 2003; 3:23–35.
18. Gordon S, Taylor PR. Monocyte and macrophage heterogeneity. Nature Rev. 2005; 5:953–964.
19. Amalfitano A, Chamberlain JD. The *mdx*-amplification-resistant mutation system assay, a simple and rapid polymerase chain reaction-based detection of the *mdx* allele. Muscle Nerve. 1996; 19:1549–1553. [PubMed: 8941268]
20. Nguyen HX, Tidball JG. Expression of a muscle-specific, nitric oxide synthase transgene prevents muscle membrane injury and reduces muscle inflammation during modified muscle use in mice. J Physiol. 2003; 550:347–356. [PubMed: 12766242]
21. Vandesompele J, De Preter K, Pattyn F, Poppe B, Van Roy N, De Paepe A, Speleman F. Accurate normalization of real-time quantitative RT-PCR data by geometric averaging of multiple internal control genes. Genome Biol. 2002; 3:RESEARCH0034. [PubMed: 12184808]
22. Carnwath JW, Shotton DM. Muscular dystrophy in the *mdx* mouse: histopathology of the soleus and extensor digitorum longus muscles. J Neurol Sci. 1987; 80:39–54. [PubMed: 3612180]
23. Bantly AD, Gray BD, Breslin E, Weinstein EG, Muirhead KA, Ohlsson-Wilhelm BM, Moore JS. CellVue Claret, a new far-red dye, facilitates polychromatic assessment of immune cell proliferation. Immunol Invest. 2007; 36:581–605. [PubMed: 18161520]
24. Horan PK, Slezak SE. Stable cell membrane labelling. Nature. 1989; 340:167–168. [PubMed: 2662017]
25. Gomez CM, Maselli R, Gundeck JE, Chao M, Day JW, Tamamizu S, Lasalde JA, McNamee M, Wollmann RL. Slow-channel transgenic mice: a model of postsynaptic organellar degeneration at the neuromuscular junction. J Neurosci. 1997; 17:4170–4179. [PubMed: 9151734]
26. Shearer JD, Richards JR, Mills CD, Caldwell MD. Differential regulation of macrophage arginine metabolism: a proposed role in wound healing. Am J Physiol. 1997; 272:E181–E190. [PubMed: 9124321]
27. Witte MB, Barbul A. Arginine physiology and its implication for wound healing. Wound Repair Regen. 2003; 11:419–423. [PubMed: 14617280]
28. Curran JN, Winter DC, Bouchier-Hayes D. Biological fate and clinical implications of arginine metabolism in tissue healing. Wound Repair Regen. 2006; 14:376–386. [PubMed: 16939563]
29. Mosser DM. The many faces of macrophage activation. J Leukoc Biol. 2003; 73:209–212. [PubMed: 12554797]
30. Porter JD, Khanna S, Kaminski HJ, Rao JS, Merriam AP, Richmonds CR, Leahy P, Li J, Guo W, Andrade FH. A chronic inflammatory response dominates the skeletal muscle molecular signature in dystrophin-deficient mdx mice. Hum Mol Genet. 2002; 11:263–272. [PubMed: 11823445]
31. Wehling-Henricks M, Jordan MC, Gotoh T, Grody WW, Roos KP, Tidball JG. Arginine metabolism by macrophages promotes cardiac and muscle fibrosis in *mdx* muscular dystrophy. PloS One. 2010; 5:e10763. [PubMed: 20505827]
32. Kalovidouris AE, Plotkin Z, Graesser D. Interferon-gamma inhibits proliferation, differentiation, and creatine kinase activity of cultured human muscle cells. II. A possible role in myositis. J Rheumatol. 1993; 20:1718–1723. [PubMed: 8295184]
33. Cheng M, Nguyen MH, Fantuzzi G, Koh TJ. Endogenous interferon-gamma is required for efficient skeletal muscle regeneration. Am J Physiol Cell Physiol. 2008; 294:C1183–1191. [PubMed: 18353892]
34. Kelic S, Olsson T, Kristensson K. Interferon-gamma promotes proliferation of rat skeletal muscle cells in vitro and alters their AChR distribution. J Neurol Sci. 1993; 114:62–67. [PubMed: 8433099]
35. Fisher PB, Miranda AF, Babiss LE, Pestka S, Weinstein IB. Opposing effects of interferon produced in bacteria and of tumor promoters on myogenesis in human myoblast cultures. Proc Natl Acad Sci U S A. 1983; 80:2961–2965. [PubMed: 6574466]
36. Mishra DK, Fridén J, Schmitz MC, Lieber RL. Anti-inflammatory medication after muscle injury. A treatment resulting in short-term improvement but subsequent loss of muscle function. J Bone Joint Surg Am. 1995; 77:1510–1519. [PubMed: 7593059]
37. Vignaud A, Cebrian J, Martelly I, Caruelle JP, Ferry A. Effect of anti-inflammatory and antioxidant drugs on the long-term repair of severely injured mouse skeletal muscle. Exp Physiol. 2005; 90:487–495. [PubMed: 15728135]

38. Shen W, Li Y, Tang Y, Cummins J, Huard J. NS-398, a cyclooxygenase-2-specific inhibitor, delays skeletal muscle healing by decreasing regeneration and promoting fibrosis. Amer J Pathol. 2005; 167:1105–1117. [PubMed: 16192645]

39. Bondesen BA, Mills ST, Pavlath GK. The COX-2 pathway regulates growth of atrophied muscle via multiple mechanisms. Amer J Physiol Cell Physiol. 2006; 290:C1651–1659. [PubMed: 16467402]

40. Mackey AL, Kjaer M, Dandanell S, Mikkelsen KH, Holm L, Døssing S, Kadi F, Koskinen SO, Jensen CH, Schrøder HD, Langberg H. The influence of anti-inflammatory medication on exercise-induced myogenic precursor cell responses in humans. J Appl Physiol. 2007; 103:425–431. [PubMed: 17463304]

41. Kirschner J, Schessl J, Schara U, Reitter B, Stettner GM, Hobbiebrunken E, Wilichowski E, Bernert G, Weiss S, Stehling F, Wiegand G, Müller-Felber W, Thiele S, Grieben U, von der Hagen M, Lütschg J, Schmoor C, Ihorst G, Korinthenberg R. Treatment of Duchenne muscular dystrophy with ciclosporin A: a randomized, double-blind, placebo-controlled multicentre trial. Lancet Neurol. 2010; 9:1053–1059. [PubMed: 20801085]

42. Chin ER, Olson EN, Richardson JA, Yang Q, Humphries C, Shelton JM, Wu H, Zhu W, Bassel-Duby R, Williams RS. A calcineurin-dependent transcriptional pathway controls skeletal muscle fiber type. Genes Dev. 1998; 12:2499–2509. [PubMed: 9716403]

43. Dunn SE, Burns JL, Michel RN. Calcineurin is required for skeletal muscle hypertrophy. J Biol Chem. 1999; 274:21908–21912. [PubMed: 10419511]

44. Semsarian C, Wu MJ, Ju YK, Marciniec T, Yeoh T, Allen DG, Harvey RP, Graham RM. Skeletal muscle hypertrophy is mediated by a Ca2+-dependent calcineurin signalling pathway. Nature. 1999; 400:576–581. [PubMed: 10448861]

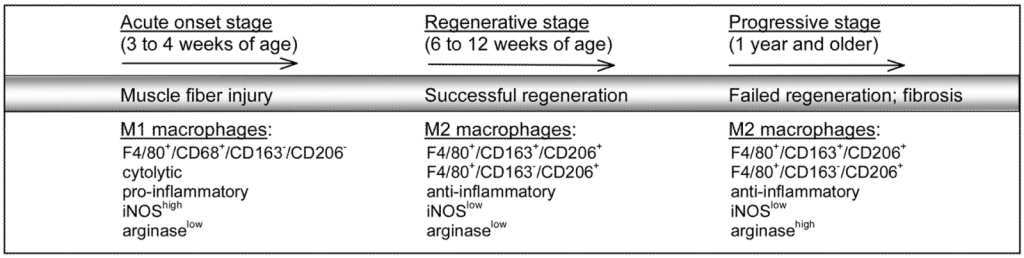

Figure 1.
Schematic of time course of *mdx* muscle pathology and changes of predominant macrophage phenotype (4, 10, 11, 15, 31, 40).

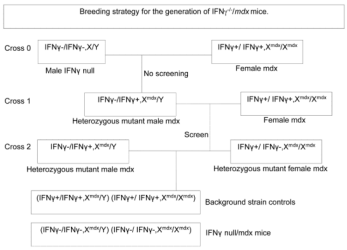

Figure 2.
Diagram of breeding strategy used to generate IFN$\gamma^{-/-}$/*mdx* mice and background strain controls.

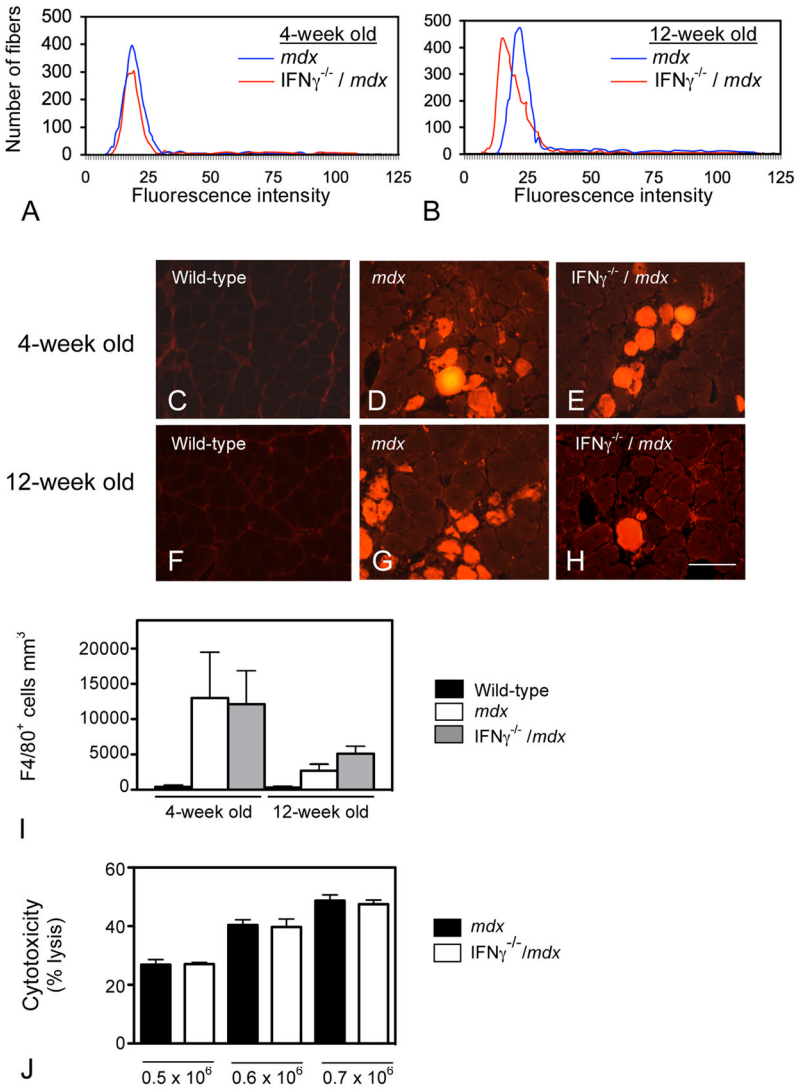

Figure 3.

IFNγ promotes muscle fiber membrane damage in 12-week-old *mdx* mice. A, B: The intracellular fluorescence intensity of muscle fibers in muscle incubated in a fluorescent, extracellular marker dye, procion orange, was used as an index of muscle fiber membrane damage. Five mice were analyzed in each data set. At 4-weeks of age (A), there is no difference between the mean, cytosolic fluorescent intensity of *mdx* fibers (blue) and IFNγ$^{-/-}$/*mdx* fibers (red). At 12-weeks of age (B), intracellular fluorescence intensity of muscle fibers in IFNγ$^{-/-}$/*mdx* muscles was less than in *mdx* muscles indicating that IFNγ promotes muscle fiber injury during the regenerative stage of dystrophinopathy. Wild-type C57 muscle fibers showed no intracellular fluorescence above background levels, which were set at the value "0" (4). C–H: representative images of soleus muscles used to quantify muscle fiber injury are shown for each group. Bar = 100 μm. I: No significant differences in the numbers of F4/80+ macrophages occurred between IFNγ$^{-/-}$/*mdx* and *mdx* muscles at either 4-weeks or 12-weeks of age. Each sample is a muscle from a separate mouse for each genotype and age-group: 4-week-old wild-type (n = 5), 4-week-old *mdx* (n = 5), 4-week old IFNγ$^{-/-}$/*mdx* (n = 5), 12-week-old wild-type (n = 5), 12-week-old *mdx* (n = 5), 12-week old IFNγ$^{-/-}$/*mdx* (n = 5). Error bars = standard error of the mean (*sem*). J: Cytotoxicity assays to

assess macrophage-mediated lysis of muscle cells *in vitro* show that macrophages isolated from muscles of 12-week-old *mdx* mice are unaffected by IFN$\gamma^{-/-}$ mutation. Each bar represents the mean of 3 samples.

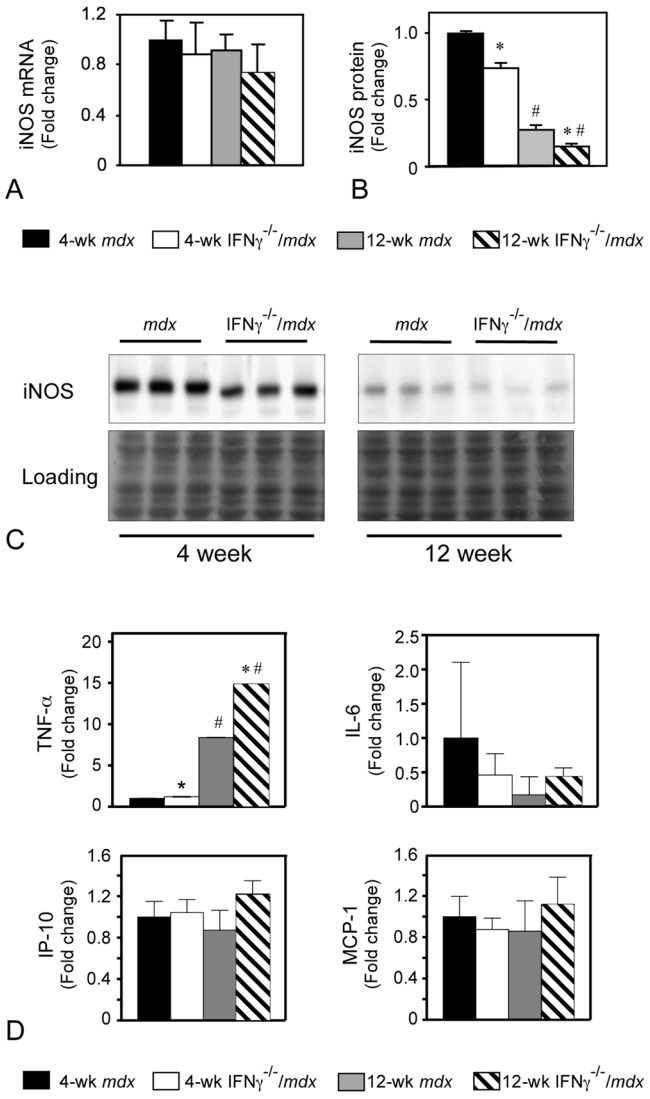

Figure 4.

IFNγ null mutation decreases iNOS expression of muscle macrophages isolated from 4-week-old and 12-week-old *mdx* mice. A: Hindlimb muscles were used for RNA isolation and qPCR for iNOS expression. Data show that iNOS mRNA levels do not change significantly between 4 and 12-weeks-of-age in either *mdx* or IFNγ$^{-/-}$/*mdx* muscles and that ablation of IFNγ expression has no effect on iNOS mRNA levels at either age. Each bar represents the mean and *sem* for the muscles collected from 5 mice in each data set. B, C: Macrophages that were isolated from hindlimb muscles of *mdx* mice or IFNγ$^{-/-}$/*mdx* mice were assayed by western blotting for relative levels of iNOS expression. Membranes were stained with Ponceau red before antibody-binding to confirm equal loading of the gel ("Loading"). Densitometry of the western blots shows that iNOS concentration declines in *mdx* mice between 4 weeks and 12 weeks of age, and that ablation of IFNγ$^{-/-}$ reduces iNOS in muscle at both ages. Each sample consists of total muscle macrophages isolated from the hindlimbs of one mouse. * indicates significantly different from age-matched sample at $p < 0.05$. # indicates significantly different from mice of same genotype at 4-weeks of age. Each bar represents the mean and *sem* of the western blot for 3 samples per data set. D: Q-PCR data for transcripts associated with M1 macrophage activation in RNA isolated from muscle

samples. Each bar represents the mean and *sem* for the muscles collected from 5 mice in each data set. * indicates significantly different from age-matched sample at $p < 0.05$. # indicates significantly different from mice of same genotype at 4-weeks of age.

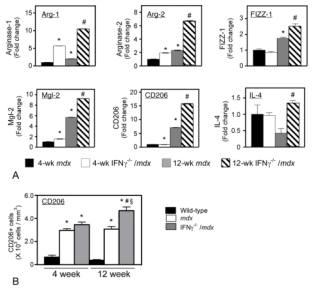

Figure 5.

IFNγ represses the expression of genes associated with M2 macrophage activation during regeneration. A: Transcript levels of M2-associated genes were measured by qPCR for RNA isolated from hindlimb muscles. Each bar represents the mean and *sem* for the muscles collected from 5 mice in each data set. * indicates significantly different from age-matched sample at $p < 0.05$. # indicates significantly different from mice of same genotype at 4-weeks of age. B. Density of CD206+ macrophages in quadriceps muscles. Data show that the number of CD206+ macrophages is elevated in dystrophic muscles and that ablation of IFNγ in *mdx* muscles further elevates CD206+ cells in 12-week-old *mdx* muscles, but not in 4-week-old *mdx* muscles. Each bar represents the mean and *sem* for the CD206+ cell counts for the quadriceps of 5 mice. * indicates significantly different from age-matched, wild-type sample at $p < 0.05$. # indicates significantly different from mice of same genotype at 4-weeks of age. § indicates significantly different from *mdx* mice at same age.

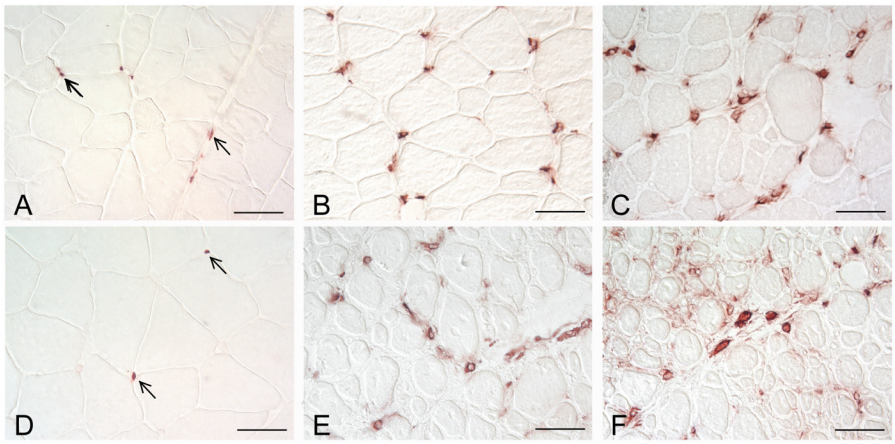

Figure 6.

Mdx dystrophy causes increases in the size of M2 macrophages and the level of activation of M2 macrophages. A: Section of a 4-week-old wild-type quadriceps muscle showing the presence of few, small CD206+ macrophages (arrows) within the endomysium between muscle fibers. B, C. The numbers and size of CD206+ macrophages (red) in muscle increases greatly in muscular dystrophy in 4-week-old *mdx* mice (B) and 4-week-old IFNγ$^{-/-}$/*mdx* mice (C). D. Section of 12-week-old, wild-type muscle. CD206+ macrophages are indicated by arrows. E, F. Sections of 12-week-old, *mdx* muscle (E) and 12-week-old IFNγ$^{-/-}$/*mdx* muscle (F) showing large CD206+ macrophages (red) within a region of muscle regeneration. All micrographs are shown at the same magnification and all sections were labeled under identical conditions. Bars = 50 μm.

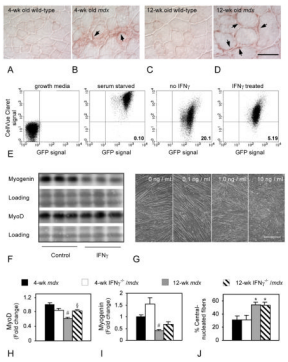

Figure 7.

IFNγ inhibits proliferation and differentiation of myogenic cells. The IFNγ receptor was expressed on the surfaces of muscle cells at higher levels in *mdx* mice at 4-weeks (B) and 12-weeks of age (D) compared to age-matched, wild-type controls (A and C). E: Flow cytometric analysis of muscle cell proliferation showed that IFNγ inhibits muscle cell proliferation of GFP-expressing C_2C_{12} cells. C_2C_{12} cells that did not express GFP and were not labeled with CellVue Claret (left panel in E) were used to set quadrant markers. F: Western blots of muscle cells treated with IFNγ or media only ("Control") *in vitro* show that IFNγ reduces the level of myogenin expression without affecting the level of MyoD expression. G. Phase contrast images of C_2C_{12} cultures show myotube growth is inhibited by IFNγ. IFNγ was added at the indicated concentrations following induction of cell differentiation and then muscle cells were incubated for 5-days to allow muscle cell differentiation and myotube growth. Bar = 160 μm. H, I: Relative transcript levels of MyoD and myogenin in whole muscle extracts were measured by qPCR. Each bar represents the mean and *sem* for the qPCR of RNA isolated from the muscles collected from 5 mice in each data set. H: MyoD expression in *mdx* muscle declined between 4 and 12-weeks-of-age. However, muscle from IFNγ$^{-/-}$/*mdx* mice showed no change in MyoD expression between these ages. I: Muscles from IFNγ$^{-/-}$/*mdx* mice showed an insignificant trend for higher levels of myogenin expression compared to *mdx* mice. J: The proportion of central-nucleated, regenerating fibers was counted and expressed as a percentage of total fibers counted in entire cross sections of soleus muscles. Each bar represents the mean and *sem* for the central-nucleated fiber counts from muscles collected from 5 mice in each data set. The proportion of regenerating fibers increased at 12 weeks, but no difference was observed between *mdx* and IFNγ$^{-/-}$/*mdx* mice at either 4 or 12 weeks of age. # indicates significantly different from 4-week-old *mdx* at $p < 0.01$. § indicates significantly different from 12-week-old *mdx* at $p < 0.01$. * indicates significantly different from 4-week old mice of same genotype at $p < 0.05$.

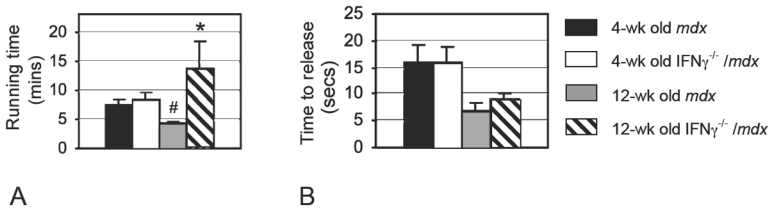

Figure 8.

Null mutation of IFNγ in *mdx* mice improves muscle function in 12-week-old mice. A: The mean maximum run time is shown for mice that ran uphill on a treadmill at a speed of 8 m/min at a 5° incline. Each sample is a separate mouse for each genotype and age-group: 4-week-old *mdx* (n = 19), 4-week old IFNγ$^{-/-}$/*mdx* (n = 18), 12-week-old *mdx* (n = 15), 12-week old IFNγ$^{-/-}$/*mdx* (n = 20). Error bars = *sem*. B: Muscle function was assessed using the wire hang test to measure front paw grip strength. Each sample is a separate mouse for each genotype and age-group: 4-week-old *mdx* (n = 20), 4-week old IFNγ$^{-/-}$/*mdx* (n = 20), 12-week-old mdx (n = 20), 12-week old IFNγ$^{-/-}$/*mdx* (n = 20). * indicates significantly different from 12-week-old *mdx* at $p < 0.05$. # indicates significantly different from 4-week-old *mdx* at $p < 0.01$.

Table 1

Primers used to assay expression levels of immune-cell and muscle-cell specific genes.

Gene	Accession Number	5′→3′		Amplicon size (bp)
IL-6	NM_031168	Fwd	GAACAACGATGATGCACTTGC	154
		Rev	CTTCATGTACTCCAGGTAGCTATGGT	
IL-4	NM_021283	Fwd	GGATGTGCCAAACGTCCTC	126
		Rev	GAGTTCTTCTTCAAGCATGGAG	
MCP-1	NM_011333	Fwd	GCTCAGCCAGATGCAGTTAAC	153
		Rev	CTCTCTCTTGAGCTTGGTGAC	
IP-10	NM_021274	Fwd	CCTCATCCTGCTGGGTCTG	165
		Rev	GTGGCAATGATCTCAACACG	
PPIA	NM_008907	Fwd	GCAAATGCTGGACCAAACAC	97
		Rev	TCACCTTCCCAAAGACCACAT	
CD206	NM_008625	Fwd	GGATTGTGGAGCAGATGGAAG	120
		Rev	CTTGAATGGAAATGCACAGA	
Mgl-2	NM_145137	Fwd	GTTTGCTCTAATTCCTTCCCAGTC	169
		Rev	GTCTAAAATGGCTCTTAGGGTGC	
FIZZ-1	NM_020509	Fwd	GAGACCATAGAGATTATCGTGGA	157
		Rev	CACACCCAGTAGCAGTCATC	
Arginase-1	NM_007482	Fwd	CAATGAAGAGCTGGCTGGTGT	153
		Rev	GTGTGAGCATCCACCCAAATG	
Arginase-2	NM_009705	Fwd	GAAGTGGTTAGTAGAGCTGTGTC	120
		Rev	GGTGAGAGGTGTATTAATGTCCG	
iNOS	NM_010927	Fwd	CTGCAGCACTTGGATCAG	124
		Rev	CGTACCAGGCCCAATGAG	
TNFα	NM_013693	Fwd	CTTCTGTCTACTGAACTTCGGG	163
		Rev	CACTTGGTGGTTTGCTACGAC	
MyoD	NM_010866	Fwd	GAGCGCATCTCCACAGACAG	178
		Rev	AAATCGCATTGGGGTTTGAG	
myogenin	NM_031189	Fwd	CCAGTACATTGAGCGCCTAC	163
		Rev	ACCGAACTCCAGTGCATTGC	

Table 2

Primers used to assay reference genes.

Gene	Access Number		5′→3′	Amplicon size (bp)
TPT1	NM_009429.3	Fwd	GGAGGGCAAGATGGTCAGTAG	113
		Rev	CGGTGACTACTGTGCTTTCG	
SRP14	NM_009273.4	Fwd	GAGAGCGAGCAGTTCCTGAC	196
		Rev	CGGTGCTGATCTTCCTTTTC	
RPS4X	NM_009094.1	Fwd	TGCTGGGTTTATGGATGTCA	107
		Rev	CCTCCTCCGGTGTAATACGA	
RPL13A	NM_009438.4	Fwd	CCTGCTGCTCTCAAGGTTGTT	146
		Rev	CGATAGTGCATCTTGGCCTTT	
RNSP1	NM_001080127.1	Fwd	AGGCTCACCAGGAATGTGAC	196
		Rev	CTTGGCCATCAATTTGTCCT	
EEF1A1	NM_010106.2	Fwd	TTGGTTCAAGGGATGGAAAG	217
		Rev	AGCAAAGGTAACCACCATGC	
GAPDH	NM_008084.2	Fwd	GCAAATTCAACGGCACAGTCAAG	248
		Rev	GGTACAAACACTACCCACACTTG	
HPRT1	NM_013556.2	Fwd	GCAAACTTTGCTTTCCCTGG	85
		Rev	CCACTTTTCCTGGAGAGCTTCA	
PPIA	NM_008907	Fwd	GCAAATGCTGGACCAAACAC	97
		Rev	TACACCAGAAACCCTTCCACT	